OPEN ACCESS
IOP Publishing | Songshan Lake Materials Laboratory
Letters
Materials Futures
Mater. Futures **1** (2022) 021001 (8pp)
https://doi.org/10.1088/2752-5724/ac66f5

Letter

Air exposure towards stable $Li/Li_{10}GeP_2S_{12}$ interface for all-solid-state lithium batteries

Wei Weng[1,2], Dong Zhou[1], Gaozhan Liu[1], Lin Shen[1,2], Mengqi Li[1], Xinshuang Chang[1] and Xiayin Yao[1,2,*]

[1] Ningbo Institute of Materials Technology and Engineering, Chinese Academy of Sciences, Ningbo 315201, People's Republic of China
[2] Center of Materials Science and Optoelectronics Engineering, University of Chinese Academy of Sciences, Beijing 100049, People's Republic of China

E-mail: yaoxy@nimte.ac.cn

Received 27 March 2022, revised 9 April 2022
Accepted for publication 12 April 2022
Published 29 April 2022

Abstract

Moist air is a great challenge for manufacturing sulfide-based all-solid-state lithium batteries as the water in air will lead to severe decomposition of sulfide electrolytes and release H_2S gas. However, different with direct reaction with water, short-period air exposure of $Li_{10}GeP_2S_{12}$ sulfide electrolyte with controlled humidity can greatly enhance the stability of $Li_{10}GeP_2S_{12}$ against lithium metal, thus realizing stable $Li_{10}GeP_2S_{12}$ based all-solid-state lithium metal batteries. During air exposure, partial hydrolysis reaction occurs on the surface of $Li_{10}GeP_2S_{12}$ pellets, rapidly generating a protective decomposition layer of $Li_4P_2S_6$, GeS_2 and Li_2HPO_3 in dozens of seconds. This ionically conductive but electronically insulation protecting layer can effectively prevent the severe interface reaction between $Li_{10}GeP_2S_{12}$ and lithium metal during electrochemical cycling. The Li/40s-air-exposed $Li_{10}GeP_2S_{12}$/Li cell shows long cycling stability for 1000 h. And the $LiCoO_2$/40s-air-exposed $Li_{10}GeP_2S_{12}$/Li batteries present good rate capability and long cyclic performances, showing capacity retention of 80% after 100 cycles.

Supplementary material for this article is available online

Keywords: $Li_{10}GeP_2S_{12}$, lithium metal, interface stability, air-exposure treatment, all-solid-state lithium batteries

* Author to whom any correspondence should be addressed.

Future perspectives

$Li_{10}GeP_2S_{12}$ is a promising solid electrolyte with high ionic conductivity and good lithium dendrite inhibition for application in all-solid-state lithium metal batteries. However, $Li_{10}GeP_2S_{12}$ can be easily reduced by lithium metal with formation of mixed conductive decomposition products including Li_2S, Li_3P and Ge/Li-Ge alloy, resulting in continuously increased interfacial impedance until cell failure. Interestingly, a stable $Li_{10}GeP_2S_{12}$/Li metal interface can be constructed simply by exposing the $Li_{10}GeP_2S_{12}$ pellet in air for dozens of seconds, and the insight reason comes from the formed ionically conductive but electronically insulated decomposition products from $Li_{10}GeP_2S_{12}$ and water in air, making the fabrication process for $Li_{10}GeP_2S_{12}$ solid electrolyte in the low-dew-point drying room possible in the future. Inspired by the air treatment strategy, further works can focus on the reactions between solid electrolytes and various gas sources to generate stable interface layers with high ionic conductivity, and thus realizing high-performance all-solid-state lithium batteries with excellent rate capability and cycling stability.

1. Introduction

All-solid-state lithium batteries exhibit increased safety due to the employment of nonflammable inorganic solid electrolytes [1–3]. To date, various inorganic solid electrolytes, especially sulfide solid electrolytes, possessing high ionic conductivity have been developed [4–8], potentially achieving high-rate capability of all-solid-state lithium batteries. However, sulfide solid electrolytes exhibit extremely poor air stability and long-time air exposure leads to severe decomposition of sulfide electrolytes with destroyed structure and release of toxic H_2S gas [9, 10]. The accumulated decomposition products with poor ionic conductivity deteriorate the bulk and interface ion transfer, and finally resulting in rapid battery decay [10, 11].

Compared with commercial lithium-ion batteries, the employment of lithium metal anodes is an essential prerequisite to realize higher energy density all-solid-state batteries [2, 3, 12]. Among sulfide electrolytes, $Li_{10}GeP_2S_{12}$ possesses high ionic conductivity of 12 mS cm^{-1}, which exceeds to that of organic liquid electrolytes [4]. However, the sulfide solid electrolyte $Li_{10}GeP_2S_{12}$ strongly reacts with lithium metal and decomposes to $Li_{15}Ge_4$, Li_3P and Li_2S [13–15]. The large fraction of metallic $Li_{15}Ge_4$ at the Li/$Li_{10}GeP_2S_{12}$ interface can create electronically conducting pathways, which will continuously consume the bulk $Li_{10}GeP_2S_{12}$ and increase impedance until cell failure. Thus, a passivating layer without electronic conductivity is crucial to suppress the highly reactive Li/$Li_{10}GeP_2S_{12}$ interface. Modification of lithium metal through chemical reaction is an appealing strategy to stabilize the Li/$Li_{10}GeP_2S_{12}$ interface. Zhang *et al* [16] identified the *in-situ* formation of the LiH_2PO_4 by reacting the lithium metal with H_3PO_4. This LiH_2PO_4 layer is ionically conducting but electronically insulating, which can prevent the direct contact between $Li_{10}GeP_2S_{12}$ and lithium metal and passivate the interface reaction. A more effective approach is introducing an electronic insulating layer with high interface energy against lithium. Wan *et al* [17] constructed a bifunctional layer at Li/$Li_{10}GeP_2S_{12}$ interface by reacting the lithium meal with $Mg(TFSI)_2$-LiTFSI-DME liquid electrolyte. The sequential reduction of salts and solvent generates a gradient solid electrolyte interface Li_xMg/LiF/polymer, resulting in a stabilized interface and demonstrating effective protection for $Li_{10}GeP_2S_{12}$. In addition, using bilayer composite electrolyte can also passivate the Li/$Li_{10}GeP_2S_{12}$ interface [18–20]. The cells employing Li-argyrodites $Li_{5.5}PS_{4.5}Cl_{1.5}$ or $Li_{10}GeP_2S_{12}$ exhibit distinct failure behavior toward lithium metal due to short circuit by lithium dendrite penetration for $Li_{5.5}PS_{4.5}Cl_{1.5}$ and increased overpotential by electrolyte decomposition for $Li_{10}GeP_2S_{12}$. The bilayer construction of Li/$Li_{5.5}PS_{4.5}Cl_{1.5}$/$Li_{10}GeP_2S_{12}$ shows excellent interface stability even at high current density, in which the $Li_{5.5}PS_{4.5}Cl_{1.5}$ layer as buffer layer is to isolate $Li_{10}GeP_2S_{12}$ from lithium metal and the $Li_{10}GeP_2S_{12}$ can prevent the lithium dendrite penetration [20]. Clearly, designing an artificial passivation interface layer by more convenient method is crucial to stabilize Li/$Li_{10}GeP_2S_{12}$ interface, while the reported approaches generally involve complicated reaction process or electrolyte multilayer structures.

Considering the severe reaction between sulfide electrolytes and moisture in air, interestingly, it is found that short-period air exposure of sulfide electrolytes with controlled humidity could provide effective passivation against lithium metal. The dramatically improved interface stability between $Li_{10}GeP_2S_{12}$ solid electrolyte and lithium metal is achieved by simply exposing the $Li_{10}GeP_2S_{12}$ pellet into air for dozens of seconds. This air-exposure treatment could rapidly generate a protective layer of $Li_4P_2S_6$, GeS_2 and Li_2HPO_3 coated on the surface of the $Li_{10}GeP_2S_{12}$ pellets. This protecting layer is ionically conductive but electronically insulation, which can not only physically isolate the contact between $Li_{10}GeP_2S_{12}$ and lithium metal but also effectively suppress the continuous decomposition of $Li_{10}GeP_2S_{12}$ reduced by lithium metal.

2. Methods

2.1. Preparation of $Li_{10}GeP_2S_{12}$ pellets with and without air-exposure treatment

The synthesis of $Li_{10}GeP_2S_{12}$ solid electrolytes can be found elsewhere [21]. The room temperature ionic conductivity of 6.13×10^{-3} S cm^{-1} and its X-ray diffraction (XRD) pattern is shown in figure S1 (available online at stacks.iop.org/MF/1/021001/mmedia). The $Li_{10}GeP_2S_{12}$ pellet (10 mm diameter, ~1 mm thickness) was prepared by cold pressing ~150 mg of $Li_{10}GeP_2S_{12}$ powder under 180 MPa. For the air-exposure treatment of $Li_{10}GeP_2S_{12}$ electrolytes, both side of the $Li_{10}GeP_2S_{12}$ pellet were separately exposed to air in a constant temperature of 30 °C and humidity chamber with 45% humidity for different durations. Before one side of the $Li_{10}GeP_2S_{12}$ pellet was exposed to air, the other side was sealed to avoid secondary exposure. Air-exposed

$Li_{10}GeP_2S_{12}$ electrolytes with duration of 40 s is labeled as 40 s air-exposed $Li_{10}GeP_2S_{12}$.

2.2. Materials characterization

To identify the composition of interfacial layer of the air-exposed $Li_{10}GeP_2S_{12}$ pellets, XRD measurements were performed on Bruker D8 Advance Diffractometer with Cu $K\alpha$ radiation ($\lambda = 1.54178$ Å). The EIS measurements for the symmetric cells were tested using Solartron 1470E electrochemical workstation (Solartron Public Co., Ltd) from 1 MHz to 0.1 Hz under 10 mV at 25 °C. Surface and cross-section morphology of $Li_{10}GeP_2S_{12}$ pellet before and after air exposure were investigated by a scanning electron microscope (Regulus-8230, Hitachi).

2.3. Electrochemical performance measurements

The lithium metal foils with thickness of 80 μm were used as electrode to assemble the symmetric cells and solid-state lithium metal batteries. To prepare the Li metal symmetric cells, two pieces of metallic lithium foils were attached on both sides of the electrolyte pellet and vacuum sealed in a pouch bag. Then the cells were isostatically pressed under 50 MPa for 5 min. The stainless steel attached with nickel tag was used as current collector. For testing the impedance of the symmetric cells after cycling tests, the galvanostatic Li plating/stripping was performed at 0.1 mA cm^{-2} and 0.1 mAh cm^{-2} under 25 °C. To fabricate the all-solid-state lithium metal batteries, the composite cathode was prepared by mixing $LiNbO_3$-coated $LiCoO_2$ and $Li_{10}GeP_2S_{12}$ powders with 70:30 weight ratio. The composite cathode (~2 mg cm^{-2}) powder was spread on one side of $Li_{10}GeP_2S_{12}$ pellet and pressed at 180 MPa to obtain the integrated cathode-electrolyte pellet. The lithium metal was attached on the other side of electrolyte pellet and sealed in pouch bag. Before assembling the air-exposed $Li_{10}GeP_2S_{12}$ based solid-state batteries, the side of $Li_{10}GeP_2S_{12}$ pellet integrated with cathode powder was sealed to avoid exposing to air. Charge/discharge measurements were conducted between 3.0 and 4.2 V at 25 °C using a multichannel battery test system (LAND CT-2001A, Wuhan Rambo Testing Equipment Co., Ltd).

3. Results

As shown in figure 1(a), in contrast with the nearly liner increasing Li plating/striping voltage for the symmetric Li/$Li_{10}GeP_2S_{12}$/Li cell without air-exposure treatment, the Li/air-exposed $Li_{10}GeP_2S_{12}$/Li cells show obviously sluggish increasement of the potential. The air-exposure durations were set at 10, 20, 30, 40, and 50 s. In addition, the suppressed increasement of impedance for the Li/air-exposed $Li_{10}GeP_2S_{12}$/Li cells was directly observed during the electrochemical cycling. Figure 1(b) presents the impedance of the Li/$Li_{10}GeP_2S_{12}$ or air-exposed $Li_{10}GeP_2S_{12}$/Li cells for the cycling tests. It can be clearly found that the continuously increasing impedance arising from strong reaction at Li/$Li_{10}GeP_2S_{12}$ interface was dramatically suppressed when the air-exposure treatment for $Li_{10}GeP_2S_{12}$ pellets was employed. Figure 1(c) presents the voltage of the symmetric Li/$Li_{10}GeP_2S_{12}$ or air-exposed $Li_{10}GeP_2S_{12}$/Li cells before and after cycling. The Li/$Li_{10}GeP_2S_{12}$/Li symmetric cell shows much higher polarization voltage than that of air-exposed $Li_{10}GeP_2S_{12}$ based symmetric cells before cycling, which is due to the decomposition reaction occurred once the $Li_{10}GeP_2S_{12}$ solid electrolytes contact with Li metal during assembling the symmetric cells. However, the obviously suppressed increasement of the voltage after cycling was detected after short-time exposure of 10 s. With increased air-exposure durations, such as 40 s and 50 s, the Li plating/striping voltages perform negligible increase even after 400 h cycling, which clearly demonstrates that the air-exposure treatment can effectively stabilize the Li/$Li_{10}GeP_2S_{12}$ interface. Whereas, the impedance of the Li/air-exposed $Li_{10}GeP_2S_{12}$/Li symmetric cells nearly linear increases with the air-exposure durations (figure 1(d)), which implies that the air-exposure treatment introduced a low ionically conducting layer at the interface. Moreover, the difference value of the impedance of the Li/air-exposed $Li_{10}GeP_2S_{12}$/Li cells for cycling tests ($\Delta R_t = R_{t,(400\,h)} - R_{t,(0\,h)}$) were evaluated. As presented in figure 1(e), the symmetric cells using $Li_{10}GeP_2S_{12}$ with an optimal exposure duration of 40 s exhibit the smallest value of the impedance changes, showing the decreased impedance for the Li/40 s air-exposed LGPS/Li symmetric cell after cycling. Specifically, compared with the impedance of around 660 Ω before cycling, the impedance decreases to around 487 Ω after 400 h cycling (figure 1(f)). The decreased impedance could be attributed to the improved interfacial contact between the decomposition layer and Li metal due to the volume expansion of lithium metal during repeat plating/striping processes [18].

Figure 2(a) shows the galvanostatic Li plating/striping of the Li/40 s air-exposed $Li_{10}GeP_2S_{12}$/Li and the Li/$Li_{10}GeP_2S_{12}$/Li cells. The Li/$Li_{10}GeP_2S_{12}$/Li cell shows a rapid increase in polarization voltage due to the continuous and deteriorative Li/$Li_{10}GeP_2S_{12}$ interface reaction. In contrast, the Li/40 s air-exposed $Li_{10}GeP_2S_{12}$/Li cell presents improved interface stability with small polarization voltage of 26 mV after 1000 h cycling. Moreover, the rate capability of the Li/40 s air-exposed $Li_{10}GeP_2S_{12}$/Li cell was evaluated in figure 2(b). When the current densities are set at 0.2 or 0.4 mA cm^{-2}, the polarization voltage is steady. However, gradual rise of polarization voltage was observed with increasing of current density to 0.6 and 0.8 mA cm^{-2}. Nevertheless, the Li/40 s air-exposed $Li_{10}GeP_2S_{12}$/Li cell can still stably cycle for 300 h at 0.2 mA cm^{-2} under an areal capacity of 0.5 mAh cm^{-2} (figure 2(c)).

To understand the mechanism of the protective layer for improving the Li/$Li_{10}GeP_2S_{12}$ interface stability, the composition of the formed protective layer through air-exposure

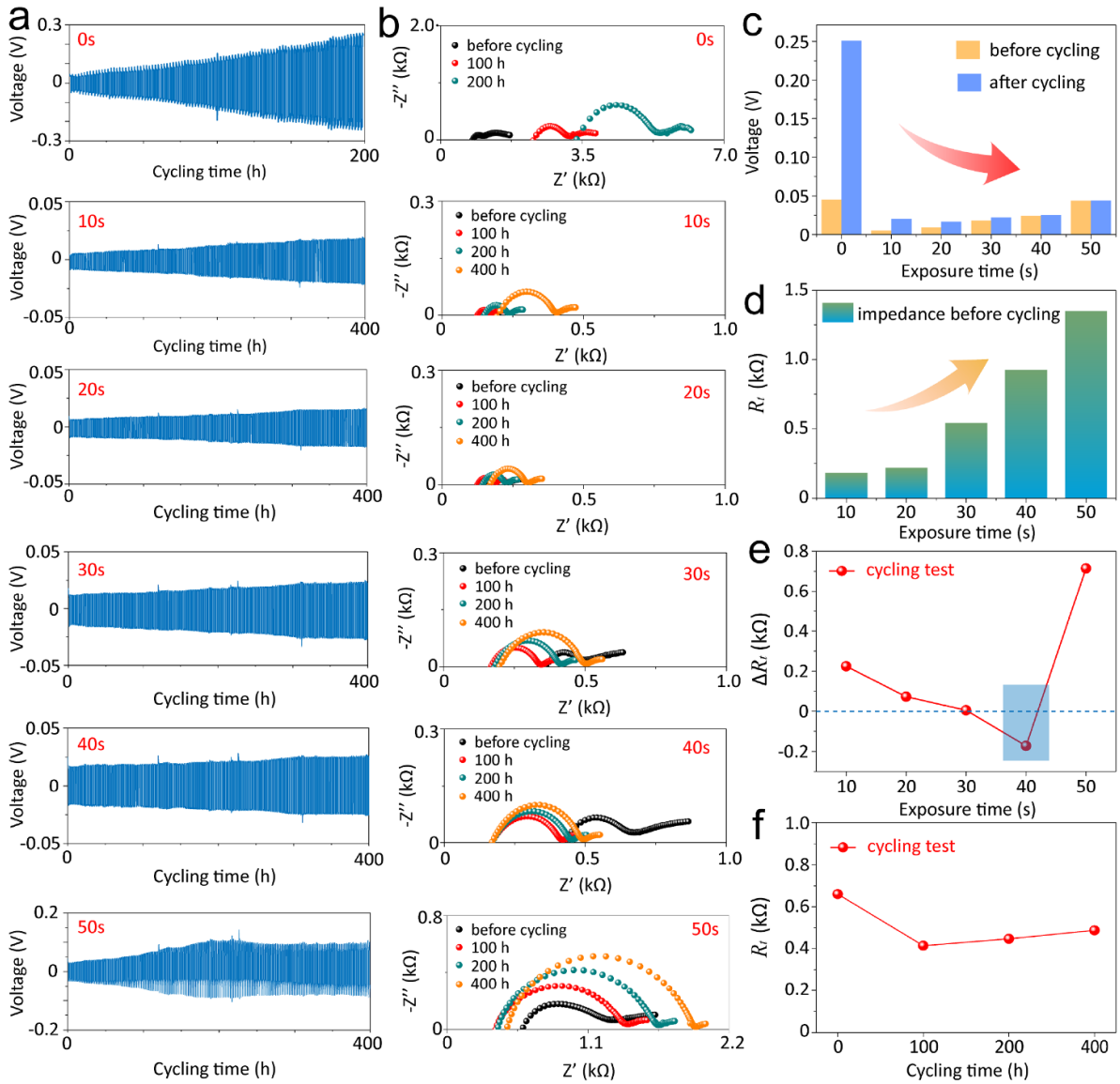

Figure 1. Evaluation of the Li/$Li_{10}GeP_2S_{12}$ interface stability through Li plating/striping experiments and evolution of impedance for the symmetric Li/$Li_{10}GeP_2S_{12}$ or air-exposed $Li_{10}GeP_2S_{12}$/Li cells. (a) Cyclic performance of the Li/$Li_{10}GeP_2S_{12}$ or air-exposed $Li_{10}GeP_2S_{12}$/Li cells at 0.1 mA cm^{-2} and 0.1 mAh cm^{-2}. (b) EIS plots of the symmetric Li/$Li_{10}GeP_2S_{12}$ or air-exposed $Li_{10}GeP_2S_{12}$/Li cells before cycling and after different cycling time. (c) Li plating/striping voltages of the Li/$Li_{10}GeP_2S_{12}$ or air-exposed $Li_{10}GeP_2S_{12}$/Li cells before and after cycling. (d) Total impedance (R_t) of the Li/air-exposed $Li_{10}GeP_2S_{12}$/Li cells before cycling. (e) Difference value of the total impedance of the Li/air-exposed $Li_{10}GeP_2S_{12}$/Li cells for cycling tests ($\Delta R_t = R_{t\,(400\,h)} - R_{t\,(0\,h)}$). (f) Evolution of the total impedance (R_t) of the Li/40 s air-exposed $Li_{10}GeP_2S_{12}$/Li cells for cycling tests.

treatment was identified. Generally, most sulfide solid electrolytes are not stable to moisture because they easily react with H_2O by release of toxic H_2S gas [10, 22, 23]. Calpa *et al* [24] reported their DFT calculation results that the hydrolysis of Li_3PS_4 would decompose into Li_3PO_4 and H_2S. Ohtomo *et al* [9] experimentally detected the Li_3PO_4 phase after the $75Li_2S{\cdot}25P_2S_5$ electrolytes reacting with water. However, the reaction products of $Li_{10}GeP_2S_{12}$ and water are unclear. Through dissolving the $Li_{10}GeP_2S_{12}$ powder into water followed by vacuum drying at 150 °C for 3 h, the reaction products are determined to be Li_3PO_4 and Li_4GeO_4, as shown in figure S2. Noticeably, the Li_3PO_4 and Li_4GeO_4 were not observed on the surface of the air-exposed $Li_{10}GeP_2S_{12}$ pellet, indicating a different reaction process occur during the air-exposure treatment. As shown in figure 3(a), for the $Li_{10}GeP_2S_{12}$ pellet after 40 s air exposure, most of diffraction peaks can be indexed to $Li_{10}GeP_2S_{12}$ phase [25, 26]. Only three diffraction peaks at 12.58°, 14.60° and 17.56° belongs to $Li_{10}GeP_2S_{12}$ phase disappear and two new diffraction peaks at 16.07° and 16.99° were detected. After 30 min

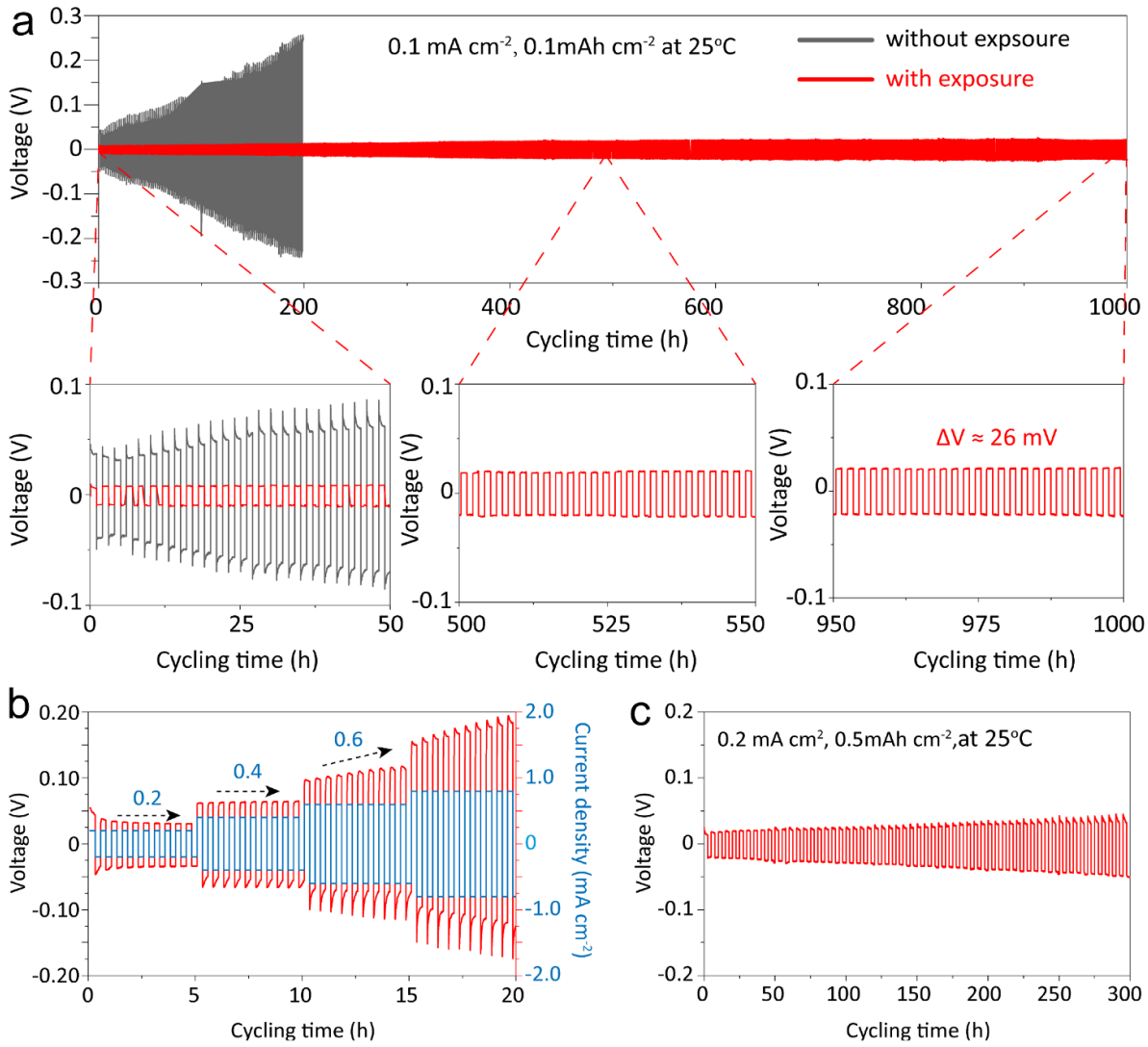

Figure 2. Galvanostatic Li plating/striping of the Li/40 s air-exposed $Li_{10}GeP_2S_{12}$/Li cells. (a) Cyclic performance of the Li/40 s air-exposed $Li_{10}GeP_2S_{12}$/Li cell at 0.1 mA cm^{-2} and 0.1 mAh cm^{-2}. The Li/$Li_{10}GeP_2S_{12}$/Li cell is also shown for comparison. (b) Rate capability at different current density and (c) cyclic performance at 0.2 mA cm^{-2} and 0.5 mAh cm^{-2} of the Li/40 s air-exposed $Li_{10}GeP_2S_{12}$/Li cell.

air exposure, large amounts of new diffraction peaks were observed, indicating new phases formed on the surface of $Li_{10}GeP_2S_{12}$ pellet. The diffraction peaks at 16.94°, 27.08°, 29.24°, 32.04°, 32.46°, 34.32°, 40.62° can be indexed to $Li_4P_2S_6$ (PDF#01-076-0992), while 15.48°, 16.94°, 26.42°, 28.82°, 31.38° belong to GeS_2 (PDF#00-030-0597) and 13.04°, 26.42°, 40.62° correspond to Li_2HPO_3 (PDF#00-035-0172). The XRD results suggest that a partial hydrolysis reaction occurs on the surface of the $Li_{10}GeP_2S_{12}$ pellet after air exposure with formation of the mixed phases of $Li_4P_2S_6$, GeS_2 and Li_2HPO_3, where the $Li_4P_2S_6$ is main phase as majority of diffraction peaks belong to it. The compound, $Li_4P_2S_6$, have been reported to exhibit considerable ionic conductivity and good interface stability towards lithium metal [27–30], making it desirable for interface protection for $Li_{10}GeP_2S_{12}$. Besides, both LiH_2PO_4 and Li_3PO_4 have been proven to be efficient protective layers for Li/solid electrolyte interface [16, 31–34], indicating phosphide, such as Li_2HPO_3, can stabilize the Li/$Li_{10}GeP_2S_{12}$ interface. Figures S3 and S4 presents the surface and cross-section morphology of $Li_{10}GeP_2S_{12}$ pellets before and after air exposure, showing the obvious decomposition layer coated on the surface of $Li_{10}GeP_2S_{12}$ pellet. Figure 3(b) presents schematic illustrations of the mechanism of the protective layer formed by air exposure for stabilizing the Li/$Li_{10}GeP_2S_{12}$ interface. For the Li/$Li_{10}GeP_2S_{12}$ interface, a mixed conductive interface is formed when $Li_{10}GeP_2S_{12}$ attaches with lithium metal, leading to continuously consume inner $Li_{10}GeP_2S_{12}$ and increase the cell impedance. After exposing $Li_{10}GeP_2S_{12}$ pellet in air, a passivating layer rapidly generated. On

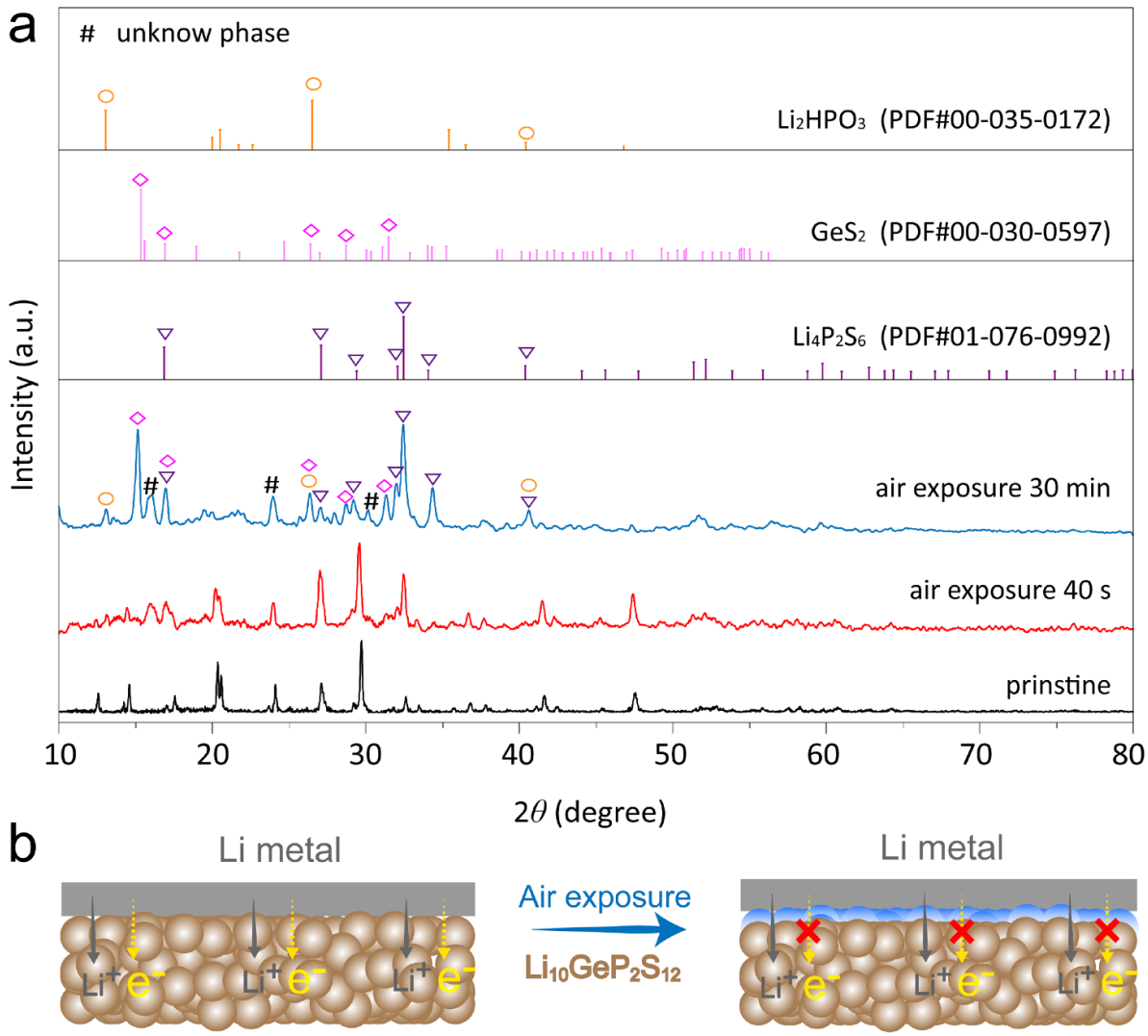

Figure 3. Improvement of the interface stability between $Li_{10}GeP_2S_{12}$ solid electrolytes and lithium metal through introducing a protective layer by air-exposure treatment. (a) XRD patterns of the $Li_{10}GeP_2S_{12}$ pellets before and after 40 s and 30 min air exposure. (b) Schematic illustrations of the mechanism of the protective layer formed by air exposure for stabilizing the Li/$Li_{10}GeP_2S_{12}$ interface.

one hand, this layer can physically isolate the $Li_{10}GeP_2S_{12}$ from lithium metal. On the other hand, this layer comprising of the $Li_4P_2S_6$, GeS_2 and Li_2HPO_3 is lithium-ion permeable but electronic obstructed, which can effectively suppress the decomposition of $Li_{10}GeP_2S_{12}$ during the Li metal plating/striping.

To further demonstrate the effect of the protective layer on stabilizing the Li/$Li_{10}GeP_2S_{12}$ interface, the $LiCoO_2$ based all-solid-state lithium metal batteries were fabricated by using both $Li_{10}GeP_2S_{12}$ and 40 s air-exposed $Li_{10}GeP_2S_{12}$ pellets as solid electrolyte. Figure 4(a) shows charge and discharge curves of the $LiCoO_2$/$Li_{10}GeP_2S_{12}$/Li battery, showing a rapid decay in specific capacity and large polarization after 5 cycles. In contrast, for the $LiCoO_2$/40 s air-exposed $Li_{10}GeP_2S_{12}$/Li battery, high reversible specific capacity and low degree of polarization are delivered (figure 4(b)). The $LiCoO_2$/40 s air-exposed $Li_{10}GeP_2S_{12}$/Li battery shows an initial charge specific capacity of 127 mA h g^{-1} with high initial Columbic efficiency of 92% and delivered long cyclic stability for 100 cycles with capacity retention of 80%, as shown in figure 4(c). The good rate performances of the $LiCoO_2$/40 s air-exposed $Li_{10}GeP_2S_{12}$/Li battery were also presented (figures 4(d) and (e)), exhibiting the discharge capacities of 113, 87, 66, 46 mAh g^{-1} at 0.1, 0.2, 0.5 and 1 C, respectively. The high reversible specific capacity and long cyclic stability strongly support the rapid generated protective layer by simple air-exposure treatment can effectively stabilize the Li/$Li_{10}GeP_2S_{12}$ interface.

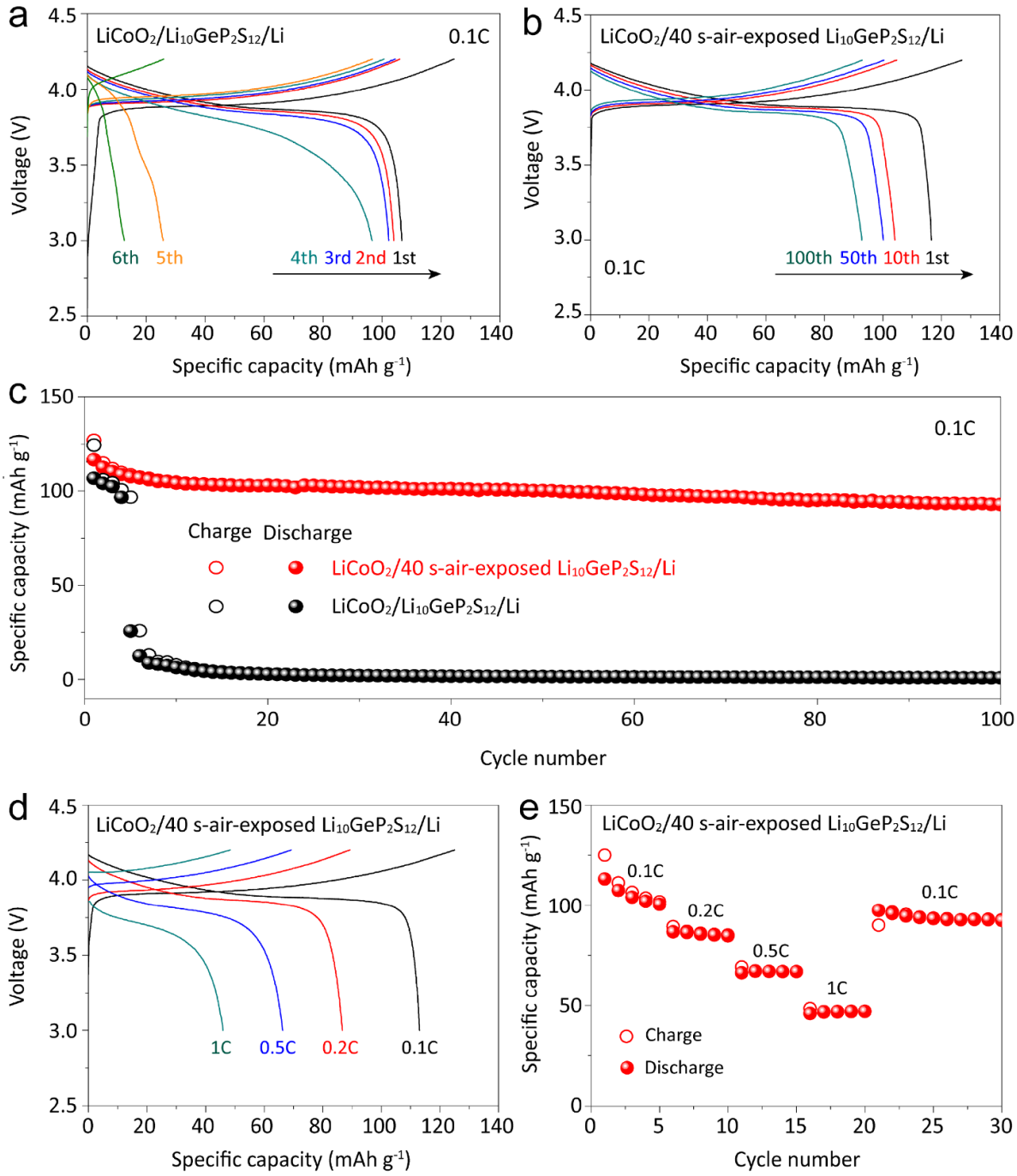

Figure 4. Electrochemical performances of all-solid-state lithium batteries. Charge and discharge curves of (a) the $LiCoO_2/Li_{10}GeP_2S_{12}/Li$ battery and (b) the $LiCoO_2$/40 s air-exposed $Li_{10}GeP_2S_{12}/Li$ battery at 0.1 C (1 C = 120 mA g^{-1}) under 25 °C. (c) Cyclic performances of the $LiCoO_2/Li_{10}GeP_2S_{12}/Li$ and $LiCoO_2$/40 s-air-exposed $Li_{10}GeP_2S_{12}/Li$ batteries at 0.1 C under 25 °C. (d) Charge and discharge curves and (e) cyclic performances of the $LiCoO_2$/40 s-air-exposed $Li_{10}GeP_2S_{12}/Li$ battery at different rates.

4. Conclusion

In summary, the strong reactive $Li/Li_{10}GeP_2S_{12}$ interface was effectively passivated via a rapid formed protective layer through simply exposing the $Li_{10}GeP_2S_{12}$ pellet to air for dozens of seconds. The protective layer coated on the surface of the $Li_{10}GeP_2S_{12}$ pellets is derived from the partial hydrolysis reaction of $Li_{10}GeP_2S_{12}$ in air, generating the decomposition products of $Li_4P_2S_6$, GeS_2 and Li_2HPO_3. This lithium-ion permeable but electronic obstructed layer can both separate the contact and effectively suppress the decomposition reaction between $Li_{10}GeP_2S_{12}$ and lithium metal during

electrochemical cycling. After optimal air-exposure duration of 40 s, the Li/40 s air-exposed $Li_{10}GeP_2S_{12}$/Li symmetric cell presents long cyclic stability for 1000 h with small polarization voltage of 26 mV at 0.1 mA cm^{-2}. Compared with the $LiCoO_2$/$Li_{10}GeP_2S_{12}$/Li battery with rapid capacity decay after 10 cycles, the all-solid-state $LiCoO_2$/40 s air-exposed $Li_{10}GeP_2S_{12}$/Li battery shows long cyclic performances for 100 cycles with capacity retention of 80%, and good rate capabilities of discharge capacity of 113, 87, 66, 46 mAh g^{-1} at 0.1, 0.2, 0.5 and 1 C, respectively.

Acknowledgments

The work was supported by the National Key R&D Program of China (Grant No. 2018YFB0905400), the National Natural Science Foundation of China (Grant Nos. U1964205, 51872303, 51902321 and 52172253), Zhejiang Provincial Key R&D Program of China (Grant No. 2022C01072), Ningbo S&T Innovation 2025 Major Special Programme (Grant Nos. 2019B10044 and 2021Z122) and Youth Innovation Promotion Association CAS (Y2021080).

Conflict of interest

The authors declare that they have no known competing financial interests or personal relationships that could have appeared to influence the work reported in this paper.

Authors contributions

Wei Weng: investigation, methodology, formal analysis, data curation, visualization, writing–original draft. Dong Zhou: visualization, validation. Gaozhan Liu, Lin Shen: methodology, visualization. Mengqi Li, Xinshuang Chang: validation. Xiayin Yao: conceptualization, supervision, project administration, funding acquisition, resources, writing–review and editing.

ORCID iD

Xiayin Yao https://orcid.org/0000-0002-2224-4247

References

[1] Janek J and Zeier W G 2016 *Nat. Energy* **1** 16141
[2] Schnell J, Günther T, Knoche T, Vieider C, Köhler L, Just A, Keller M, Passerini S and Reinhart G 2018 *J. Power Sources* **382** 160–75
[3] Randau S *et al* 2020 *Nat. Energy* **5** 259–70
[4] Kamaya N *et al* 2011 *Nat. Mater.* **10** 682–6
[5] Seino Y, Ota T, Takada K, Hayashi A and Tatsumisago M 2014 *Energy Environ. Sci.* **7** 627–31
[6] Bachman J C *et al* 2016 *Chem. Rev.* **116** 140–62
[7] Meesala Y, Jena A, Chang H and Liu R S 2017 *ACS Energy Lett.* **2** 2734–51
[8] Zhang Z Z *et al* 2018 *Energy Environ. Sci.* **11** 1945–76
[9] Ohtomo T, Hayashi A, Tatsumisago M and Kawamoto K 2013 *J. Mater. Sci.* **48** 4137–42
[10] Liang J *et al* 2020 *Chem. Mater.* **32** 2664–72
[11] Ye L, Gil-González E and Li X 2021 *Electrochem. Commun.* **128** 107058
[12] Lee H, Oh P, Kim J, Cha H, Chae S, Lee S and Cho J 2019 *Adv. Mater.* **31** e1900376
[13] Han F D, Zhu Y Z, He X F, Mo Y F and Wang C S 2016 *Adv. Energy Mater.* **6** 1501590
[14] Wenzel S, Randau S, Leichtweiss T, Weber D A, Sann J, Zeier W G and Janek J 2016 *Chem. Mater.* **28** 2400–7
[15] Zhu Y, He X and Mo Y 2015 *ACS Appl. Mater. Interfaces* **7** 23685–93
[16] Zhang Z, Chen S, Yang J, Wang J, Yao L, Yao X, Cui P and Xu X 2018 *ACS Appl. Mater. Interfaces* **10** 2556–65
[17] Wan H, Liu S, Deng T, Xu J, Zhang J, He X, Ji X, Yao X and Wang C 2021 *ACS Energy Lett.* **6** 862–8
[18] Yao X Y, Huang N, Han F D, Zhang Q, Wan H L, Mwizerwa J P, Wang C S and Xu X X 2017 *Adv. Energy Mater.* **7** 1602923
[19] Wan H, Liu G, Li Y, Weng W, Mwizerwa J P, Tian Z, Chen L and Yao X 2019 *ACS Nano* **13** 9551–60
[20] Ye L and Li X 2021 *Nature* **593** 218–22
[21] Yin J, Yao X, Peng G, Yang J, Huang Z, Liu D, Tao Y and Xu X 2015 *Solid State Ion.* **274** 8–11
[22] Shang S L, Yu Z, Wang Y, Wang D and Liu Z K 2017 *ACS Appl. Mater. Interfaces* **9** 16261–9
[23] Kimura T, Kato A, Hotehama C, Sakuda A, Hayashi A and Tatsumisago M 2019 *Solid State Ion.* **333** 45–49
[24] Calpa M, Rosero-Navarro N C, Miura A, Jalem R, Tateyama Y and Tadanaga K 2021 *Appl. Mater. Today* **22** 100918
[25] Kwon O, Hirayama M, Suzuki K, Kato Y, Saito T, Yonemura M, Kamiyama T and Kanno R 2015 *J. Mater. Chem.* A **3** 438–46
[26] Culver S P, Squires A G, Minafra N, Armstrong C W F, Krauskopf T, Bocher F, Li C, Morgan B J and Zeier W G 2020 *J. Am. Chem. Soc.* **142** 21210–9
[27] Dietrich C, Sadowski M, Sicolo S, Weber D A, Sedlmaier S J, Weldert K S, Indris S, Albe K, Janek J and Zeier W G 2016 *Chem. Mater.* **28** 8764–73
[28] Nagata H and Akimoto J 2020 *ChemistrySelect* **5** 9926–31
[29] Stamminger A R, Ziebarth B, Mrovec M, Hammerschmidt T and Drautz R 2020 *RSC Adv.* **10** 10715–22
[30] Suyama M, Yubuchi S, Deguchi M, Sakuda A, Tatsumisago M and Hayashi A 2021 *J. Electrochem. Soc.* **168** 060542
[31] Zhang H *et al* 2021 *Angew. Chem., Int. Ed.* **60** 19183–90
[32] Shi Y N, Zhou D, Li M Q, Wang C, Wei W, Liu G Z, Jiang M, Fan W T, Zhang Z H and Yao X Y 2021 *ChemElectroChem* **8** 386–9
[33] Niu J J, Wang M M, Cao T C, Cheng X P, Wu R, Liu H, Zhang Y F and Liu X Q 2021 *Ionics* **27** 2445–54
[34] Zheng G R *et al* 2020 *Energy Storage Mater.* **29** 377–85